5

RFID Antennas – Possibilities and Limitations

Johan Sidén and Hans-Erik Nilsson
Mid Sweden University / Sensible Solutions Sweden AB
Sweden

1. Introduction

Marking items for remote identification not only places high demands on the heart of the RFID tags, the Application Specific Circuit (ASIC), but also on the tag antennas. For long reading distances, efficient antennas are crucial and their efficiency is directly proportional to the maximum reading distance of both semi-active and passive tags.
This chapter is an in-depth investigation of the requirements for the antenna part of UHF RFID tags, with focus on antenna design, characterization and optimization from the perspectives of both costs involved and technical constraints. The main focus is devoted to antennas that could be manufactured using more or less standard manufacturing techniques available in the packaging industry. The chapter also presents some new ideas on how to utilize the antenna structure itself as a sensor for measuring different physical properties during the logistic chain.
The chapter starts by describing the most general requirements for a functional UHF antenna, explaining why designs for RFID tag antennas cannot be taken directly from traditional antennas designed for other applications since RFID chips input impedances differ significantly from traditional input impedances such as 50 Ω and 75 Ω.
Ordinary antennas, not made for RFID, are usually also designed to work at a particular location or at locations where the surroundings of the antenna are well known. This is not generally the case for RFID applications, where the antenna is largest part of the tag and where the near field region of the antenna will be defined by the object and material that the RFID tag is attached to. For cost and practical reasons, tag antennas should be two-dimensional and if they are applied to paper or soft plastics they should be non-sensitive to bending, particularly as they might be placed over an edge of an object. An antenna's resonant length is also directly dependent on its surrounding medium. If the antenna is designed to be placed in free space it will change its properties if placed next to a dielectric medium, even if this medium is electrically lossless. There is thus a demand for some kind of general tag antennas and guidelines for designing and optimizing tag antennas when their final location is known in advance. The type of antenna properties and designs to be avoided are similarly given as well as which types should be used when, for example, putting antennas onto flexible, dielectric and metallic materials. Specific solutions presented also include how to enhance the tags' commercial value by incorporating insignias such as company logos in the antenna design.
Antennas used in traditional RFID tags are mainly made out of copper or aluminum. In order to keep the antenna prices to a minimum and facilitate very large production it is desirable to fabricate the tag antennas using commercially available web shaping techniques

Source: Radio Frequency Identification Fundamentals and Applications, Design Methods and Solutions, Book edited by: Cristina Turcu, ISBN 978-953-7619-72-5, pp. 324, February 2010, INTECH, Croatia, downloaded from SCIYO.COM

or utilizing printing processes with electrically conductive ink. Conductance in such prints is normally based upon relatively expensive silver particles and for cost reasons, printed antennas should therefore have as small a total printed area as possible, thin trace thickness and still be robust and maintain high radiation efficiency. The chapter therefore includes a discussion and examples of the trade-off between cost and antenna performance when minimizing the amount of expensive material by thinning the printing layers.
For tagging objects containing materials that cause problems to one layer antennas and where traditional double layer PCB antennas are too expensive to use, we will also show how microstrip antennas can be manufactured using printing processes and cardboard material as substrate.
The chapter, with its regards to efficiency of RFID tag antennas, ends with a presentation of how pairs of ordinary low-cost passive RFID tags can be used as remote reading sensors and specifically moisture sensors. This is possible by arranging one antenna in such a way that it degrades in performance in proportion to the physical quantity it is designed measure and letting the other antenna serve as reference. For use as moisture sensors this is easily done by embedding one of two identical RFID tags in moisture absorbing material and leaving the other tag open. If the pair of tags are placed in a humid environment or directly exposed to wetness the embedded tag will require a higher minimum signal strength than the open tag to operate. The differences involved in reading the two tags are proportional to the level of humidity or wetness and the pair of tags in this setup can thus be used as low-cost remote sensors and similar setups can be used for remote measurements of other quantities.

2. Design of a simple one-layer RFID tag antenna

The RF front of passive RFID chips often incorporates Schottky diodes, which give rise to an input impedance far from that commonly seen in other RF systems [1]. Schottky diodes are used to rectify incoming RF signals to supply power to the RFID chip. They are also used to modulate the signal reflected by the antenna back to the reader. To obtain as high as possible feed voltage to the chip, a voltage doubler is usually implemented with the aid of two Schottky diodes. The input impedance observed by the antenna therefore has a relatively low real part and an imaginary capacitive part of some hundred Ohms. An example of Schottky diodes that could be used for this purpose involves the Agilent Technologies' HSMS-282x Series [2]. These diodes feature low series resistance, low forward voltage at all current levels, and good RF characteristics. Considering a voltage doubler built using Schottky diodes at the chip's RF input, the impedance observed by the tag antenna can be described as two parallel Schottky diodes. Through the use of the equations presented in the data sheet of the mentioned diodes, the impedance for one diode can be calculated to 72– j×244 Ω for the frequency 868 MHz, assuming room temperature, and an operating current 25 μA. Two parallel diodes thus give a chip impedance of 36 – j×122 Ω. To maximize power transfer from the antenna to the chip, a conjugate impedance match is required [1], which in this case implies that the antenna should have an input impedance, Z_A, close to 36 + j×122 Ω.
Looking at the Smith Chart for the most basic antenna, the half wavelength dipole, in Fig. 1 (a) and (c), one sees that this kind of antenna cannot be tuned to the desired input impedance by simply adjusting its length. The same dipole equipped with an inductive load in parallel to the antenna input terminals can however reach this order of input impedance as is illustrated in Fig. 1(b) and (d). The ordinary dipole antenna in Fig. 1 (a) has dimensions

l=163 mm, *w*=2 mm and *g*=1 mm and the inductive dipole in Fig. 1 (b) has dimensions *l*=185 mm, loop length *ll*=20, loop height *lh*=10 mm and line width *lw*=1 mm. Both Smith charts in Fig. 1 are achieved by simulating the antenna patterns in Ansoft HFSS [3] and sweeps from 500 MHz to 1500 MHz where the markers indicate the frequency and 868 MHz.

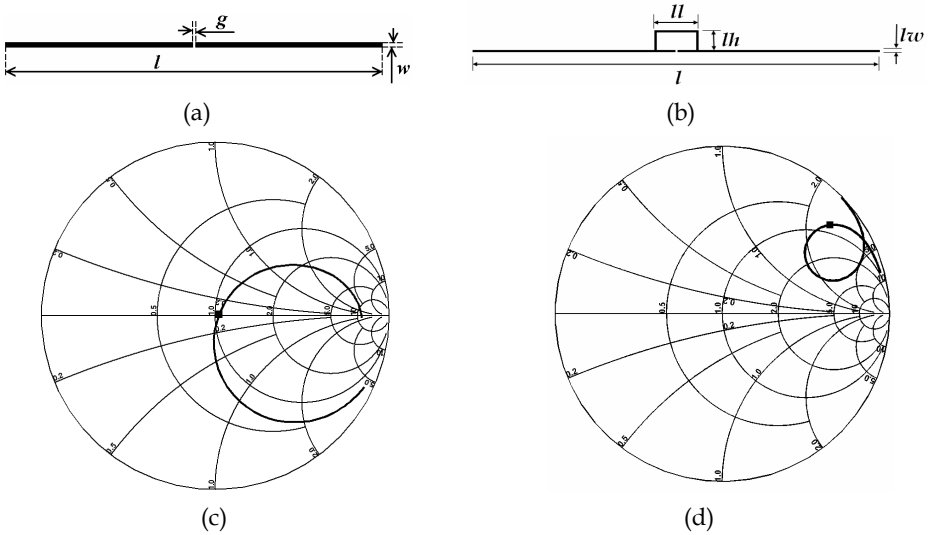

Fig. 1. An ordinary dipole (a) and (b) the same with an additional loop to make its input impedance more inductive. (c) and (d) show the Smith Charts of respectively the antennas in (a) and (b)

3. Printed antennas

Printed antennas are considered in order to reach an RFID technology fully integrated into packaging fabrication lines. The drawback with printed antennas, however, is their reduced radiation efficiency as compared to their copper counterparts as the bulk conductivity of their printed traces is lower than for solid metals. This chapter shows how careful antenna design and proper printing technologies can produce antennas which are as efficient as copper antennas and how this can be accomplished using a minimum of conductive ink.

3.1 Radiation efficiency of a printed antenna

Metallic conducting particles, which are usually in the shape of flakes or spheres, are blended into an ink vehicle and printed, for example, by means of a flexographic printing press. Conductivity is created by the overlap of the conductive particles, which is why the bulk conductivity is naturally lower than for solid metals.

Different printing technologies can be utilized to apply ink onto different substrates, for example flexography, gravure, screen-printing and Inkjet. Inkjet printing however requires expensive nano-sized particles and the printing speed of ink-jet systems is still lagging behind other techniques. Naturally, we will see technology breakthroughs in the area of ink-jet technology and this technique cannot be neglected in the future.

As mentioned, the main drawback of printed antennas is their limited conductivity when compared to fabricating antennas from solid metals. Basic laws for conductors and conductivity state that ohmic losses decrease as conductor thickness increases [4]. Even though printed ink traces are not homogenous, a similar behavior will also apply to this case. An electrical transmission line of a given length and width, and printed with a particular ink thickness, has a total resistance proportional to the length and inversely proportional to the trace width and thickness.
In the industry, flexographic printers are commonly multi-station units, containing up to ten stations in a series, where each station usually prints one color (Fig. 2). With identical printing plates and the same silver ink at several stations, a multi-station flexographic printer can also be used to print ink layers whose thickness is proportional to the number of stations used. In the specific laboratory printer setup used, the experience has been that each print pass provides a layer thickness of the order of 3-5 μm. Using such a setup, it is possible to choose layer thicknesses as multiples of 3-5 μm by choosing the number of stations to use.

Fig. 2. Image of a multi-station flexographic printer. Printed trace thickness can be adjusted by letting two or more stations print with identical printing plates.

Losses in conductor and substrate materials are very difficult to distinguish through measurements. Even though methods for this have been proposed [5], it is even more difficult when the investigated conductor is a radiating antenna [7]. The effect of limited conductivity is initially obtained by simulating the antenna in free space, i.e. with no substrate.
Fig. 3 shows the simulated input impedance locus in a Smith Chart for the antenna in Fig. 1 (b) printed with different sheet resistances and for frequencies 500-1500 MHz where 868 MHz is marked by black dots. All simulations assume an antenna without substrate. In the Smith Chart the graph representing the antenna made of a Perfect Electrical Conductor (PEC) has the widest loop, very closely followed by antennas with sheet resistances 50 and 100 mΩ/□. The antennas made with the highest sheet resistances, 1000 and 5000 mΩ/□, have narrower loops as the sheet resistance increases. A narrower loop, caused by higher ohmic losses, is an indication of the antenna receiving a lower Q-value. A lower Q-value also implies a wider bandwidth, which is observed as a shorter total distance in the Smith Chart traversed by the graph for higher sheet resistances. For higher sheet resistance the whole graph is also translated towards both higher resistance and lower reactive values, and would eventually occur in the rightmost part of the Smith Chart, i.e. the higher the sheet resistance of the antenna structure, the more similar it is to an open end transmission line.

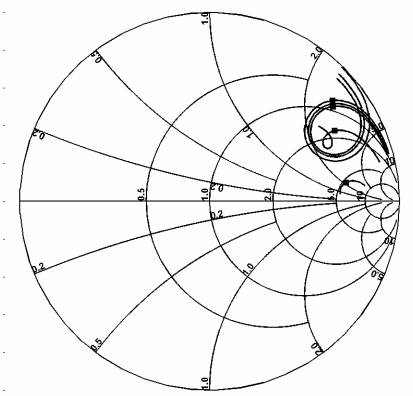

Fig. 3. Smith chart from simulations of antennas in free space and with sheet resistances 0 (PEC), 50, 100, 1000, and 5000 mΩ/□ respectively, with the higher sheet resistances corresponding to smaller loops. Frequency spans from 500 MHz at the upper end of graphs to 1.50 GHz at the lower end. 868 MHz is marked with black dots.

Since the input impedance is changed when ohmic losses are introduced, there will also be losses caused by an impedance mismatch. The efficiency of power transferred to, or received by, the antenna due to a non-perfect impedance match can according to [7] be expressed as

$$e_{mismatch} = 1 - |\Gamma|^2 = 1 - \left| \frac{Z_A - Z_C^*}{Z_A + Z_C} \right|^2 \quad (1)$$

where Γ is the voltaic reflection due to impedance mismatch, Z_A is the antenna input impedance and Z_C is the chip impedance. Maximum power transfer from the antenna to the chip occurs when Z_A and Z_C are the complex conjugates of each other, i.e. $Z_A=Z_C^*$. Table I shows the calculated radiation efficiency due to a mismatch using Equation (1) and the impedance values are presented in the same table. It is assumed that the antenna is originally designed to be fabricated as a PEC, placed in free space, and has a perfect impedance match for this PEC. The complex conjugate of the PEC antennas input impedance is therefore set as the reference chip impedance, Z_C. Mismatch due to some potential substrates is discussed in the next section.

Sheet Resistance (mΩ/□)	Input Impedance	Radiation Efficiency due to Mismatch	Radiation Efficiency due to Ohmic Loss	Total Conductor Radiation Efficiency $e_{Conductor} = e_{Mismatch} \cdot e_{Ohmic}$
PEC	*38 + j130 Ω*	100 %	100 %	100 %
50	39 + j121 Ω	99 %	85 %	85 %
100	41 + j118 Ω	99 %	76 %	75 %
1000	60 + j96 Ω	84 %	24 %	21 %
5000	86 + j70 Ω	43 %	4 %	2 %

Table I. Simulated Radiation Efficiency due to Limited Conductivity

From Table I it is obvious that as long as it is possible to print this antenna with sheet resistances below 100 mΩ/□, the radiation efficiency due to an impedance mismatch is almost negligible with $e_{Mismatch}$ above 99 %. It is observed that 100 mΩ/□ corresponds to a printed layer thickness of approximately 5 μm, and can be achieved by only one pass with the flexographic printer used while two passes are preferable. More important is the size of the ohmic losses which are introduced to the system due to the ink conductivity, and how this affects the total radiation efficiency. Ohmic loss is the part of the power that is absorbed in the antenna and converted into heat. The efficiency due to ohmic losses, e_{Ohmic}, is therefore defined as the quotient between radiated power, $P_{Radiated}$, and antenna input power, P_{in} [7]:

$$e_{Ohmic} = \frac{P_{Radiated}}{P_{in}} \tag{2}$$

The radiation efficiency due to ohmic losses is also retrieved from the same simulations as used to calculate the input impedance, and as presented in Table I. It is seen that ohmic losses are a much more severe contribution to loss in radiation efficiency, than that introduced by an impedance mismatch. For instance, a sheet resistance of 100 mΩ/□ gives a mismatch efficiency $e_{Mismatch}$=99 %, but the ohmic efficiency is only e_{Ohmic}=80 %. The total radiation efficiency of the printed antenna, $e_{Conductor}$, due to both impedance mismatch and ohmic losses is the product of the two loss quantities as shown in Equation (3)[7].

$$e_{conductor} = e_{Mismatch} \cdot e_{Ohmic} \tag{3}$$

The result of (3) is placed in the last column of Table I, where the print of for example 100 mΩ/□ gives a total radiation efficiency of $e_{Conductor}$ =75 %.

3.2 Radiation efficiency due to substrate loss

While the previous section characterized losses due to a printed antenna's limited conductivity, focus is now switched to potential losses introduced by common printer substrates and final objects subject to RFID tagging. Three different substrates are considered, a thin glossy paper, a plastic film, and a thick paper, all with the potential to be used as an antenna substrate in a commercial printing press. The complex permittivity of the substrate materials were measured using an Agilent 8507 Dielectric Probe Kit, together with an Agilent E5070B Vector Network Analyzer, and can be read in Table II.

Material	Thin Paper	Plastic Film	Thick Paper
Thickness (μm)	87	73	600
Relative Permittivity at 868 MHz	4.01 0 j0.29	1.89 + j0.059	2.2 + j0.14
Loss Tangent	0.07	0.031	0.064

Table II. Measured Substrate Permittivities

To only characterize the effect of substrate losses, and not the antenna conductor losses, the antenna is now regarded as a PEC in the simulations, with no ohmic losses due to antenna conductivity. Fig. 4 shows the simulated input impedance results, for the same antenna as before on the introduced substrates. The substrates behaved in a very similar manner, and

the frequency 868 MHz is again marked by black dots. Referring to the dots' relative positions, the thick paper is the upper left, thin paper the middle and plastic film the lower right.

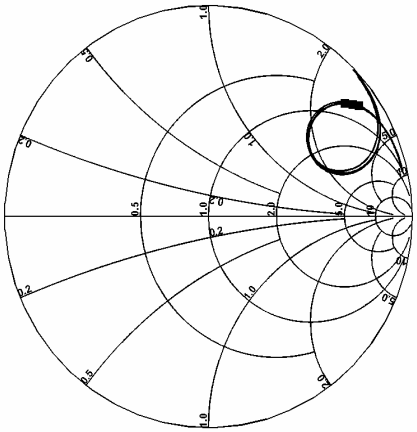

Fig. 4. Smith chart for antenna made of PEC on the substrates thin paper, thick paper and plastic film.

Substrate	Radiation Efficiency due to Mismatch	Radiation Efficiency due to Ohmic Loss	Total Radiation Efficiency $e_{Substrate} = e_{Mismatch} \cdot e_{Ohmic}$
Thin Paper	95 %	96 %	92 %
Plastic Film	99 %	99 %	98 %
Thick Paper	89 %	93 %	84 %

Table III. Radiation Efficiency due to Introduced Substrate

In a manner similar to the investigations involving finite conductivity in the previous section, Table III quantifies losses introduced by substrates in terms of the impedance mismatch and ohmic losses respectively. These losses may not be considered severe, with the worst case being the thick paper that shows a total radiation efficiency due to substrate of $e_{Substrate}$=84 %. According to Table III, the best substrate in this situation is the plastic film with an $e_{Substrate}$=98 %. As it is known from the previous section, lower ohmic losses produce wider loops in the Smith Chart but this can hardly be discerned in Fig. 4, since the substrate losses are relatively low. When comparing radiation efficiency in Table III to the Smith chart in Fig. 4, it should however be kept in mind that if a specific substrate is considered in the antenna design process, the efficiency due to a mismatch could approximate to 100 %. The ohmic losses are quite low, even though the substrates' loss tangents are significantly above zero. As seen in Table III that the plastic film, with the lowest loss tangent, also produces the lowest ohmic losses. The low ohmic losses are mostly due to the low substrate thickness relative to the wavelength, λ. For the thick paper for example the substrate thickness is about 0.0018 λ. If the substrate were to be thicker, but with the same relative permittivity, both the mismatch and ohmic losses would increase as will be shown in section 5.

3.3 Total radiation efficiency

Total radiation efficiency depends on ohmic and mismatch losses introduced by both the antenna conductor and substrate:

$$e_{Total} = e_{Conductor} \cdot e_{Substrate} \tag{4}$$

Table IV show the simulated total radiation efficiency for the introduced substrates, when printed with sheet resistances 50, 100, 1000, and 5000 mΩ/□, respectively. As might be expected from the results in Table I and III, the highest radiation efficiency, 83%, is achieved for 50 mΩ/□ on plastic film.

Substrate	50 mΩ/□	100 mΩ/□	1000 mΩ/□	5000 mΩ/□
Thin Paper	78 %	69 %	19 %	1.4 %
Plastic Film	83 %	74 %	20 %	1.5 %
Thick Paper	71 %	63 %	17 %	1.3 %

Table IV. Simulated Total Radiation Efficiency for different Conductivities and Substrate Materials

It has been shown that impedance mismatch is a minor contributor to the total loss for thin substrates. However, this can still be avoided by taking care in the antenna design process. If the antenna's length is changed just a couple of millimeters the impedance mismatch becomes almost negligible, while the efficiency due to ohmic losses remains almost identical, which is further discussed in section 5. These results are valid for this particular dipole and although the general trends may hold true for other designs, the relationship between conductivity and radiation efficiency is also highly dependent on the antenna design. Factors such as size, print area, slot, patch, loop, etc. will also affect the radiation efficiency.

3.4 Maximum RFID read distance

In passive RFID systems, the maximum distance at which a tag can be read is always a crucial factor. The tag's only power supply is from the interrogating radio wave, and the amplitude of this wave is strictly regulated by governmental authorities. It is well-known that the power received at a given distance from a transmitting unit is inversely proportional to the square of the transmitting distance. The amount of received power is calculated using the Friis transmission formula [4]

$$P_r = \frac{(P_t \cdot G_t) \cdot G_r \cdot \lambda^2}{(4\pi R)^2} \tag{5}$$

where R is the distance between the tag and interrogator and $P_t \cdot G_t$ the Effective Isotropic Radiated Power (EIRP) transmitted by the interrogator unit. In the US, the transmitted power allowance is 4 W EIRP, and in EU 2W ERP (= 3.28 W EIRP). G_r is the gain of the receiving tag antenna, and λ the wavelength.

As follows from Eq. (5), when the distance between the interrogator unit and the tag is doubled, power received by the tag falls by a factor of four. It also follows from the equation that in order to obtain the same power with two antennas with different total radiation

efficiencies, it is required to move the less efficient antenna closer to the interrogator by a factor of the square root of the ratio of total radiation efficiency. If, for example, a printed antenna has a total radiation efficiency of 64 % compared to the reference one made of copper (100 % radiation efficiency), the operating RFID range for a tag using the printed antenna would be approximately √0.64 • 100 % = 80 % of that for the copper one. In this way, measured sheet resistances of printed antennas can be used to characterize antenna radiation efficiency in computer simulations that in turn can be converted to predict theoretical RFID read ranges due to the square root relationship.

The presented theories were tested in reality by printing the antenna in Fig. 1(b) with a laboratory flexographic printer that was set to print multiple passes and with differently diluted ink. The measured conductivity values for the samples printed on HP photo film were between 67 and 680 mΩ/□ and RFID chips were attached and connected to the antennas with aid of manually added silver ink drops.

The maximum RFID read range was measured at an approximated (in-door) open air read range setup as illustrated in Fig. 5, where r can be varied from approximately 0 m up to 8 meters before reflections from the rightmost balcony significantly influence the measurements. The RFID system used in this experiment followed the European standard with a maximum output power of 2 W ERP. All experiments are however performed to show the relative values and normalized by the maximum reliable reading distance for a PEC dipole that was found to be about 6.4 m. The results are presented in Fig. 6 where the experimental values are slightly under the theoretical ones but have the same characteristics.

From Fig. 6 it appears that in order to achieve a decent functionality for printed RFID antennas, with the ink and printing techniques used, a sheet resistance of 100 mΩ/□ or lower is desirable. The ink thicknesses corresponding to the best antenna was measured with the aid of a Mahr Millitast 1083 Digital Indicator Gage [6] to be about 10 μm. The uncertainty in ink thickness is largely due to a deviation in paper thickness of the order of several micrometers.

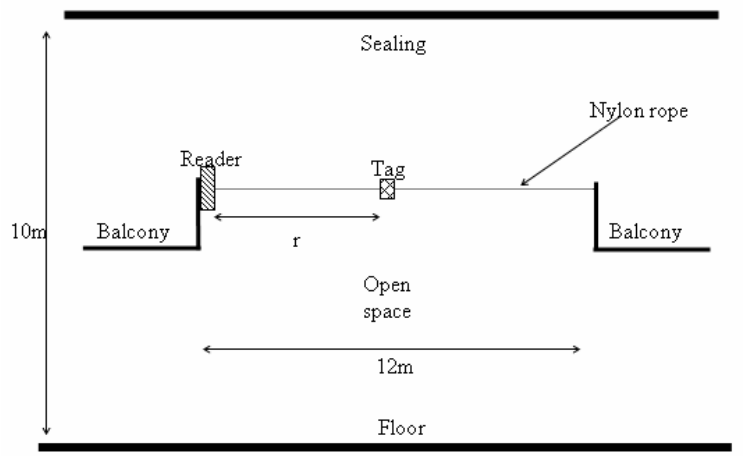

Fig. 5. Setup for determining maximum RFID read distance.

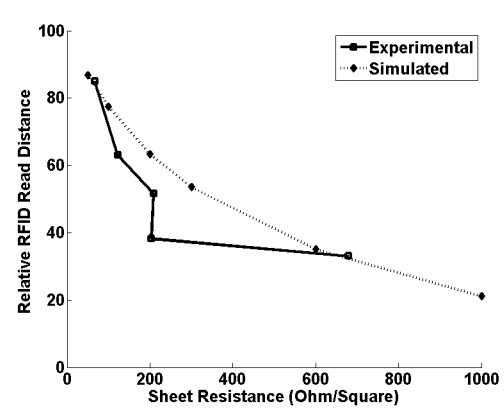

Fig. 6. Simulated and experimental values for relative RFID read range versus the sheet resistance of the printed antenna.

4. Flexible substrates and physical bending of antennas

Single layer RFID antennas on flexible substrates such as thin paper or plastics may be exposed to physical bending, especially if an RFID label is placed on a non-flat surface or over the corner of an object. This section uses numerical simulation [3] to study the impact of bending on some typical examples of RFID antennas.

The performance degradation to an RFID system caused by bending the tag antenna is investigated for the two antenna structures in Fig. 7 where the antenna in Fig. 7 (a) is relatively narrowband with a VSWR=2.0 bandwidth of 4% and the antenna in Fig. 7 (b) is a bit more wideband with bandwidth 11%. The narrowband antenna in Fig. 7 (a) is a folded dipole that is adapted to fit the impedance of passive of RFID chips by cutting a slot in the upper conductor.

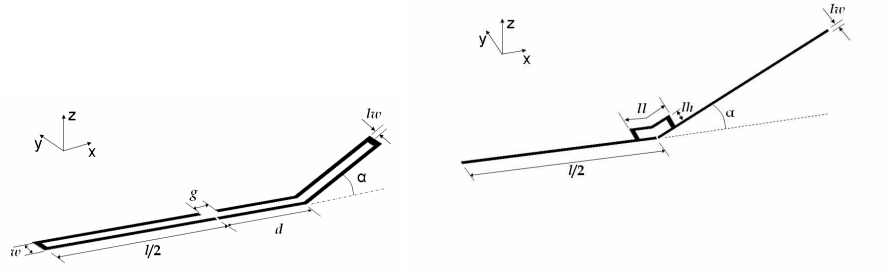

(a) (b)

Fig. 7. An antenna will change its input impedance when distorted by bending, which is numerically simulated when bent towards the z-axis for (a) a narrowband printed folded dipole with a cut in the upper conductor for RFID impedance matching and (b) a more wideband RFID dipole.

The dipoles are fed in the middle and one of the dipole arms is bent at different angles α and at different distances *d* from the feed as shown in Fig. 7. The simulated folded dipole Fig. 7 (a) has a total length of *l*=120 mm, width *w*=8 mm, gap *g*=6 mm and line width *lw*=2 mm and the dipole in Fig. 7 (b) has a total length of *l*=185 mm, loop length *ll*=20, loop height *lh*=10 mm and line width *lw*=1 mm. The input return losses of the bent folded dipole for different values of α and *d* are shown in Fig. 8 where it can be seen how the input return loss increases as the antenna is bent at a point closer to the feed. The maximum input return loss occurs when α=90° and d=0 and one can see that the wide band dipole handles this slightly better than the narrowband dipole.

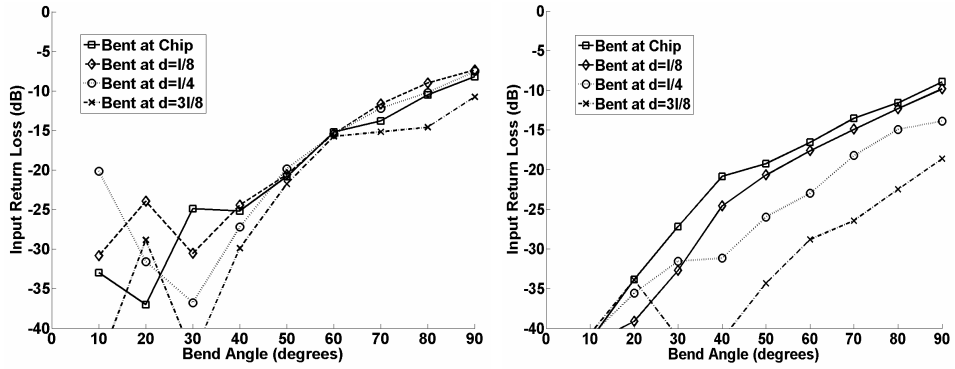

(a) (b)

Fig. 8. Input return loss of (a) narrowband dipole and (b) wideband dipole when bent at different angles α at different positions *d*.

The bending of the antenna structure will no doubt result in performance degradation to an RFID system. The amount of such degradation can be expressed in terms of relative read range according to the following formula

$$RR = \sqrt{\left(1 - |\Gamma|^2\right)\frac{D'}{D}} \tag{6}$$

where RR is the relative read range as compared to a perfectly matched RFID system with the reader antenna illuminating the tag antenna in its z-direction. Γ is the reflection coefficient due to impedance mismatch which is why $1-|\Gamma|^2$ becomes a factor that describes the relative power entering the chip. D is the tag antenna's directivity in the z-direction when flat, and D′ the directivity in the z-direction when the antenna is bent. Friis' transmission formula in equation (5) tells us that the radiated power decreases in proportion to the distance squared which is why the relative read range in equation (6) becomes the square root of the mismatch and directivity factors.

The performance degradation due to antenna distortion is provided in Fig. 9 where it is observed that the operating range will be reduced to approximately 60% for both dipoles in the worst case scenario when the dipoles are bent 90° in the middle of the structure. The wideband dipole does not outperform the narrowband here as it did in Fig. 8, the reason for this is that the directivity in the antennas' z-direction changed more for the wideband antenna than for the narrowband one.

It is also observed that when bent at d=3*l*/8 the reduction of the operating range is almost negligible. This is an interesting observation which potentially allows for improvements to the tag construction. If the RF tag substrate is to be made less flexible in the vicinity of the dipole antenna feed point, but still allowing greater flexibility at its exterior, it could significantly reduce the tag performance degradation caused by placing it on non-flat or flexible surfaces.

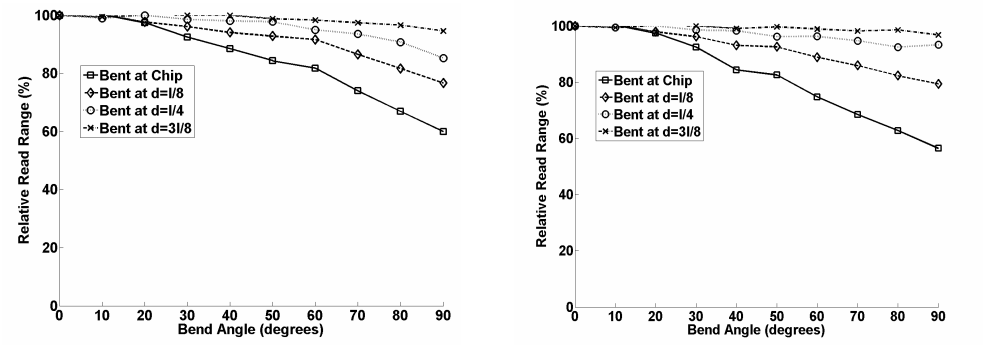

Fig. 9. Performance degradation of RFID systems for an (a) narrowband and (b) wideband dipole RFID tag antenna bent at different angles α at different distances d from the structure centre.

5. Wideband and narrowband RFID antennas behavior on background materials

As previously investigated in section 3.2, single layer RFID antennas normally have a relatively thin substrate to carry the antenna structure which does not significantly affect neither the antenna's input return loss nor its radiation efficiency. The thin carrying substrate will however place the antenna in very close proximity to other materials when applied to an object. Depending on the size of the object and the electrical properties of its material it can cause significant changes to the antenna parameters which in turn can reduce the maximum read range of the RFID tag.

Prior knowledge of the underlying material's electrical properties, losses due to impedance mismatch can to a certain degree, be compensated for in the original antenna design process by properly scaling the antenna's dimensions. Ohmic losses introduced by nearby materials can unfortunately not be compensated for by only scaling the antenna geometry but will still be present.

Pure conductive, i.e. metallic, surfaces and thick materials with very high dielectric losses, such as containers filled with water, can also be compensated for but this requires a multi-layered antenna structure which is exemplified in section 6 or the use of a spacer of a particular thickness to distance the single layer antenna from the surface.

This section shows how resonant frequency and input return loss changes when the previously used narrowband and wideband antennas in Fig. 7 were placed on a pile of paper, well representing a book, instead of the single papers investigated in section 3.2.

5.1 Changes in input return loss and radiation efficiency when put on 40 mm paper material

The paper used as substrate material has the same relative permittivity of ε_r=4.0 + j0.29 as previously but is now 40 mm thick. The simulated input return loss shown in Fig. 10 was again calculated using standard formulas for reflections due to impedance mismatch taking the input impedance of the antennas with no nearby material as the reference value.

Changes from the free space situation are obvious and it can be observed how the narrowband antenna has an input return loss of almost 0 dB when placed on the pile of paper while the wideband antenna, also out of reach, at least manages to have approximately -2 dB in the same situation. The radiation efficiency when put on the pile of paper was calculated to 26% and 65% for respectively the narrowband and wideband antenna and it was also noted that the directivity in the z-direction decreased to about 0.2 in both cases. All in all this does cause the narrowband dipole to totally malfunction but also significantly decreases the performance of the wideband dipole.

The narrowband dipole could indeed be specifically tuned to electrically fit this underlying material, but is then again only of use for that material and no other. The wideband dipole could also be geometrically adapted for optimal performance but the necessity for this is less obvious.

A dipole that inherits wideband properties is of course also beneficial for communication if a high bit-rate is desired or if a wideband-demanding modulation- and coding scheme such as a frequency hopping spread spectrum (FHSS) is to be used.

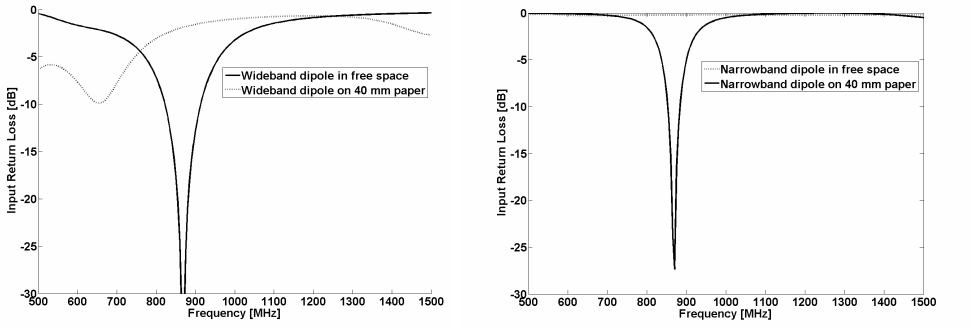

(a) (b)

Fig. 10. (a) Input return loss for the antennas in Fig. 7 (a) and (b) when operating surrounded by free space and when put on top of 40 mm paper. While the wideband dipole does increase its input return loss significantly, the narrow dipole is more or less completely malfunctioning.

5.2 Adopting the narrowband dipole for underlying material

Resonance, very close to the original impedance point, is achieved for the dipole antenna upon the pile of paper by reducing its length from 120 mm to l=70 mm and increasing its linewidth from 2mm to lw=5 mm, and its total width w from 8 mm to w=17 mm. As mentioned, the ohmic losses cannot be compensated for by simple changes in the antenna geometry but actually increases to 42%. The antenna tuned for this specific material naturally becomes detuned again if used in free space.

Tuned narrowband antennas such as the ordinary dipole can thus be used when pre-knowledge of intended nearby materials' electrical properties is available. If a final underlying material on the other hand is unknown at the time of antenna design, narrowband antennas are consequently not a good choice and should be avoided.

6. Microstrip antennas

The microstrip antenna consists of a patch of metallization on a ground plane. These are low profile and generally have a height of only a few mm. The ground plane can consist of a patch whose size is just slightly larger than the radiating patch. Microstrip antennas have the advantage that they can be made more or less transparent to the underlying material which partly solves the problem associated with the RFID tags in an unknown environment. They are however also relatively sensitive to ohmic losses in the substrate used between the patch and the ground plane which is the reason why expensive low loss microwave substrates are often used in applications requiring microstrip antennas.

6.1 Low cost microstrip antennas for passive tags on metallic objects

The performance of a conventional tag antenna is strongly degraded by metallic objects as this affects both the impedance and radiation pattern. When a general dipole-type antenna is mounted near a metallic object, a current will be induced on both the antenna surface and the metallic surface due to the RFID reader's radiation. The metallic surface acts as an image to the original antenna, which has a negative influence on the tag antenna's scattered field and makes the tag unreadable within normal ranges [10].

Antennas that can be directly used with RFID tag for metallic objects include the planar inverted-F antenna (PIFA), U slot inverted-F tag antenna [11], [12], antennas based on slots in the metallic object itself [13] and Microstrip Antennas (MSA)[14].

As the electronic identification technology competes with rock-bottom pricing barcodes, the cost involved is the most obvious issue which is holding back the widespread adoption of RFID. Fabricating efficient MSAs from low-loss microwave substrates is therefore not possible for general RFID applications. Some low cost materials, such as foam, have been used as MSA substrate for RFID [15] but no cheaper alternative solution has been proposed for the conducting parts. Unlike a conventional dipole-type antenna, the MSA is a structure with two conducting layers acting as a resonance cavity and which is thus much more sensitive to ohmic losses in the substrate and conductors than for the simple one-layer antennas investigated previously.

This section therefore investigates the performance of silver ink printed MSAs for passive RFID operating at 868 MHz. Two compact patch structures were designed where the conducting parts of the patch antenna are flexographically printed with silver ink and common cardboard is used as the substrate. One antenna consists of a solid patch and one of very wide slots in the patch in order to minimize ink usage. The aim was to design antennas that could work as well in free space as when placed on a metallic plate.

6.2 Printed MSA design

The size of the basic MSA is quite large as it should be approximately half the wavelength divided by the square root of the substrate relative permittivity in two dimensions and have a ground plane larger than the patch. MSAs for RFID must therefore be modified. It has

been demonstrated that by using a shorting plate or by cutting slots, compact MSAs can be achieved [16]. In Fig. 11.(a), a shorting plate is added to the middle of one radiating edge (the top edge). The antenna's resonance frequency is controlled by tuning the width Dp of the shorting plate, where the resonance frequency decreases with the decreasing Dp. In order to facilitate the chip mounting, a segment of microstrip line is connected to the radiating patch and a slot is cut along the feed line for the placement of an RFID chip. One end of the feed line is directly connected to the ground plane by means of a small piece of copper tape and the shorting plate is achieved by wrapping a segment of copper tape through a slot which is cut along the radiating edge, through the substrate and to the ground plane. In an industrial process line, it should be possible to substitute the small pieces of copper tape, acting as a wide via, by staples.

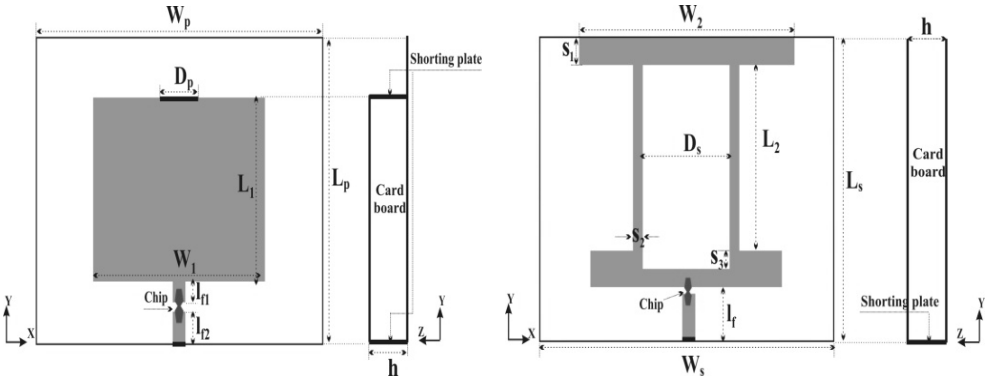

(a) (b)

Fig. 11. Geometrical Structures of (a) Shorted and (b) Slot Microstrip Patch Antenna

The shorted MSA is a compact antenna but suffers from poor gain and degradation in the radiation pattern. An alternative method of reducing the resonance frequency of the MSA is to increase the patch length of the surface current by cutting slots in the radiating patch. Generally, size reduction is achieved by adopting a C-shaped or H-shaped slot or a ring MSA [16]. In order to make the antenna more compact, both the H-shaped slot and ring are adopted in this case, resulting in the geometry shown in Fig. 11 (b). Slots are respectively cut in the middle and along the two non-radiating edges of the patch. As with the shorted MSA in Fig. 11 (a), a segment of microstrip line is used to feed the slot patch and the RFID chip is placed across the gap between the feed line and patch. The connection between the feed line and the ground plane is also achieved by the same method as that for the shorted MSA. In both cases, corrugated cardboard with a thickness of approximately 2.8mm is utilized as the substrate. The electrical properties of the cardboard material, i.e. complex permittivity parameters, could unfortunately not be measured due to lack of equipment but it would have been interesting.

The ground plane, radiating patch and feed line were flexographically printed [17] with three consecutive passes onto a plastic film with a thickness of 80μm using the silver based ink CFW-102X [18]. After being cured at 120°C for 20 minutes, an average DC sheet resistance of 70mΩ/□ was obtained. The plastic films holding the printed traces were glued to the respective sides of the cardboards. The antennas were optimized by repeated impedance and read range measurements for different dimensions with the final

geometrical parameters: Wp=100 mm, Lp=Ls=75 mm, Dp=12 mm, W1=60 mm, L1=45 mm, lf1=5 mm, lf2=9 mm, Ws=110 mm, W2=80 mm, L2=38 mm, Ds=27 mm, lf=10 mm, s1=12 mm, s2=2.5 mm, s3=9 mm.

In order to evaluate the influence of the limited conductivity of the silver ink printed conductors on the antennas performance, two copper antennas were constructed with the same geometry by replacing the printed plastic film with 70 μm thick copper film. The input impedance of the printed and copper patch antennas were measured with the vector network analyzer E5070B and the results are displayed in Fig. 12. Fig. 12 (a) shows the impedance traces of the shorted patch antennas and Fig. 12 (b) shows those involving the slots. The solid lines represent the impedance traces of copper antennas and the dashed lines are those of the printed ones. The measured frequency range is from 500 to 1500 MHz and the square shaped marks represent the impedance values at 869 MHz. In the Smith Chart it can be seen that the radius of the impedance trace circles of the printed antennas in both cases are smaller than those of the copper ones, which represents more conduction loss and is similar to that observed throughout Chapter 3.

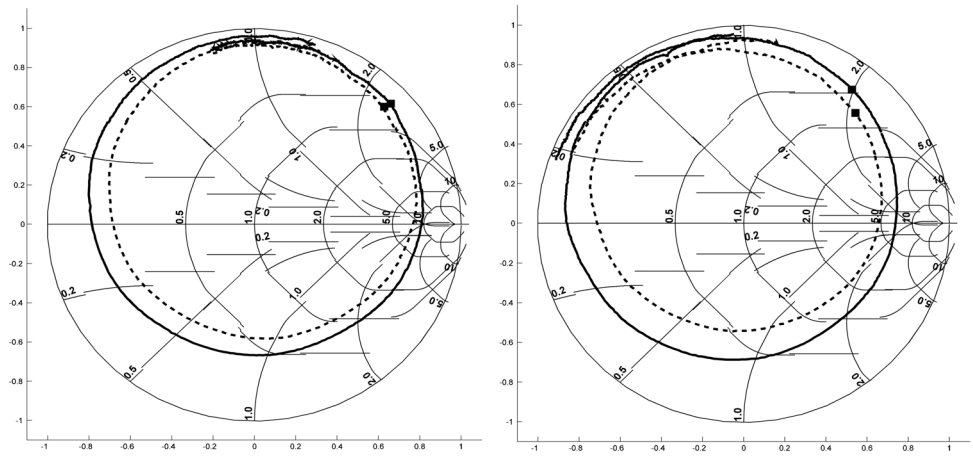

(a) (b)

Fig. 12. Measured Input Impedance of (a) Shorted and (b) Slot Patch Antennas.

It was also observed that the radius difference is more obvious for the slot patch antenna than for the shorted one which might be because of the higher current density on traces with limited conductivity.

Alien chips with straps were placed across the slots along the respective feeds. The read range in the front direction of these four tags when there are no metallic objects nearby and when they are mounted at the centre of a metallic plate of size 305×165mm is obtained by placing the tag in the approximated open air read range in Fig. 5 with the SAMSys reader operating at 2 W ERP. The results are shown in Table XIX and observed that, without any objects nearby, the read range of the slot patch antennas are better than those of the shorted ones with the metallic plate behind the slot patch. Both antennas however perform better with the metallic plate behind, which is mainly due to no back radiation. The range enhancement is also rather better for the shorted patch antenna than for the slot one. In the Smith Chart, it can be seen that the impedance values of the slot patch antennas at 869 MHz

are more close to the conjugate impedance value of the RFID chip than those of the shorted ones implying a higher input return loss for the slot patch antennas.
The read range of the copper antennas is only slightly better than the range for the printed ones and this is probably due to both lower ohmic losses and a better impedance match with the copper antennas. Since the geometrical parameters for the antenna are determined for the printed patch antennas, the input impedance will offset those of the originals when applying the same geometrical parameters to the more conductive copper antennas. This then degrades the impedance match between the antenna and the RFID chip.

Antenna type	Without metallic objects nearby	When mounted on a metallic plate with size of 305×165mm
Shorted microstrip patch antenna (copper)	2.2 m	3.3 m
Shorted microstrip patch antenna (printed)	2.0 m	2.8 m
Slot microstrip patch antenna (copper)	2.5 m	2.8 m
Slot microstrip patch antenna (printed)	2.3 m	2.4 m

Table XIX. Measured Read Range in the Front Direction of the Patch Antenna

7. Aesthetic appearance of RFID antennas

Antennas are most often designed with little or no attention to their aesthetic appearance. Typically, antennas are optimized for functionality in a specific application, or to fit within a specific footprint. RFID antennas can however be visible on packaging and products, and a graphic design could serve promotional purposes. This section shows how the adaptation of logo designs can serve as operating RFID antennas and thus add a promotional dimension to the RFID antenna design. A package, or other object, generally has a company logo or similar trademark printed on it and with the proposed concept that logo can also serve as a silver-printed RFID antenna.

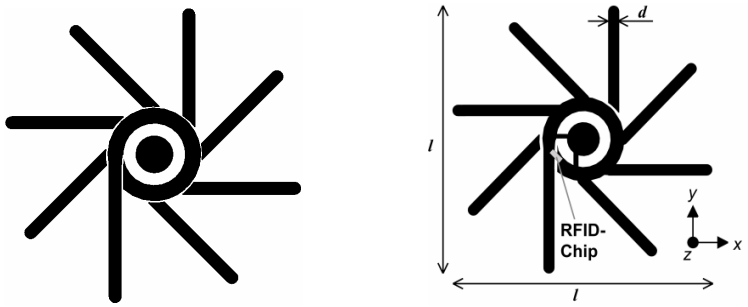

(a) (b)

Fig. 13. (a) The Precisia LLC company logo and (b) the same logo changed into an RFID tag antenna.

7.1 Converting logotypes to RFID tag antennas

To be effective, a resonant antenna must be comparable in size to the working wavelength (usually about at least one sixth of a wavelength). For UHF RFID systems, this means about 5-15 cm in size in at least one dimension, implying that they will be very visible even when placed on relatively large objects such as containers and pallets. Typical modern RFID antennas are variations of well known structures such as dipoles, loops, slots, and meander lines. Very few RFID antenna structures are designed as an artwork even though some examples exist and include a patch antenna with the slot in the shape of an adapted University logo helping to achieve higher working bandwidth [20], and a modified meander type dipole antenna, using a text pattern [21].

As shown previously common antennas such as ordinary dipoles, folded dipoles and the like are unable to be scaled to reach impedances that fit common passive UHF RFID chips unless altered by adding or removing parts. The proposed consept include converting a logotype to an antenna where one first decides where on the geometry to place the chip and then add and remove conductive parts trying to not severely distort the original artwork. If the pre-bonded chips referred to as straps are used, the feed gap could be up to 4-5 mm. A greater challenge in converting logos to antennas is if one not only considers the input impedance but is also designing for specific directivity patterns.

As flexographic printing is the most common method for printing on cardboard material all antennas chosen for this investigation were printed using a laboratory flexographic printer by RK Print [17].

7.2 The precisia company logo as RFID antenna

Fig. 13shows the original logo by Precisia LLC [18] and its version modified to become an RFID antenna template. The original logo design contains the first letter of the company name “P” with the filled circle in the middle surrounded by filled lines forming a “star”-like pattern. The loop in the letter “P” is not completely closed and the surrounding rotated lines are not connected to the “P” (there are small gaps), except for the vertical line in the “P” itself.

The process of converting the logo into a functional RFID antenna structure was initiated by choosing a placement position for the RFID chip. With the present graphical design it was decided to make the final structure as similar to the dipole as possible. In such a case, the chip should be positioned close to the geometric centre of the structure. In this particular case, the gap in the loop of the letter “P” was chosen (see Fig. 13(b)). The central filled circle was connected to the loop by two lines, forming a shorted loop connected in parallel to the chip pads. The intention of keeping such a loop close to the chip becomes clear when looking at the altered dipole antennas used in the previous sections, as it can serve as the impedance matching quasi-lumped inductor. After trial and error with Ansoft HFSS [3] some of the remaining lines in the “star” pattern were connected to the loop. Finally, the whole antenna was scaled in the structure simulator to provide operating frequency around 867 MHz with resulting dimensions l= 131 mm and d= 5 mm.

Measured input impedances of antennas made from both copper foil and flexographic print are shown in Fig. 14.

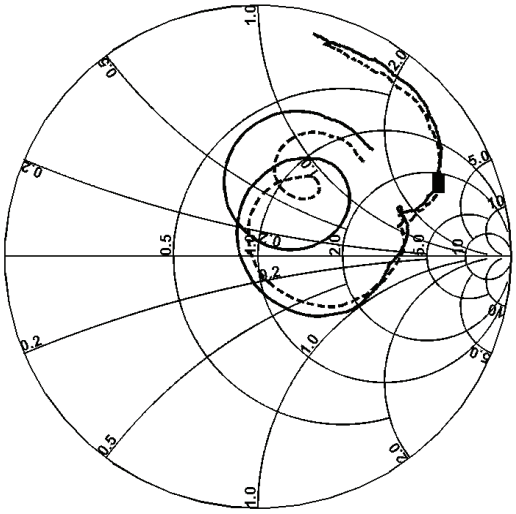

Fig. 14. Measured input impedance for the Precisia logo antenna, made from copper foil (solid line) and printed with conductive ink (dashed line). The graphs sweep from 500 to 1500 MHz and the markers on the impedance curves (the filled square) are set to 867 MHz.

The antennas were equipped with Alien Monza Gen2 chips and were measured to have maximum reliable read range of 5.16 m for the copper antenna and 4.03 m for the printed one, which can be compared 6.0 m maximum reading distance for a copper antenna very similar to the inductive dipole presented earlier.
The radiation pattern was extracted by measuring maximum read range for different angles and is shown in Fig. 15.

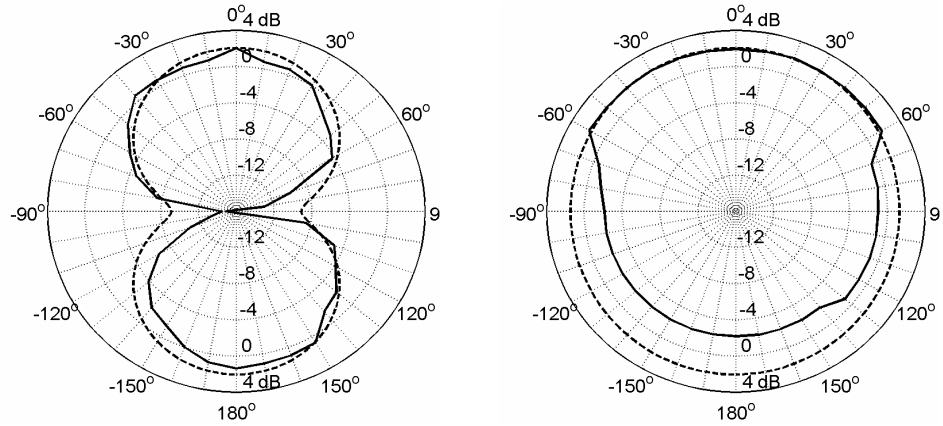

(a) (b)

Fig. 15. Measured (solid line) and simulated (dashed line) radiation patterns for the Precisia logo antenna in (a) the xz-plane and (b) the yz-plane. Maximum directivity is about 2.0 dB, directed along the z-axis

In order to demonstrate that almost any logo could be arranged as an RFID antenna some additional logos from the Michigan region were evaluated. The reading distance of these experiments are presented in Table XIII.

Antenna pattern	Antenna printed on plastic film with silver based ink	Antenna made from copper foil
Precisia Logo	4.03 m	5.16 m
Detroit Pistons	4.81 m	6.05 m
Michigan M	5.54 m	5.79 m

Table XIII. Maximum RFID Read Range for Printed and Solid Copper Antennas

8. RFID antennas as RFID sensors

Up until today, very few RFID chips exist that include an input port also for sensor data, i.e. an extra digital or analogue input port. The analogue version could for example measure the resistance over a sensor port, allowing for simple passive sensor elements that change resistance proportional to the physical quantity of interest. One application where this would be valuable is in the remote measuring of moisture or the wetness level at the location of the tag. Moisture sensor tags with costs similar to those of ordinary ID tags could for instance be placed inside walls or floors in buildings. The humidity level inside the wall could be read by holding a handheld RFID reader at, say, one meter from the wall provided that the positions of the tags are discretely marked or mapped. By periodically reading the tags it is possible to prevent costly damage due to mould or putrefaction. The tag could be advantageously positioned directly underneath hidden water pipe connections for early leakage detection.
This section presents a concept where pairs of ordinary RFID tags are exploited for use as remote reading moisture sensors by embedding one of the two tags in a moisture absorbing material.

8.1 Open and embedded tags

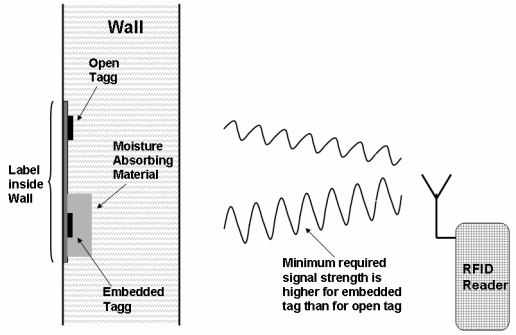

Fig. 16. Moisture sensing label incorporating two RFID tags where one of the tags is covered with a paper based moisture absorbing material. In a humid environment the embedded tag's antenna gets less efficient and needs a stronger RF signal to operate. The difference in RF power to operate is proportional to the humidity level.

Existing technologies for remote reading of humidity levels in hidden locations such as inside walls are based on different microwave technologies [22]-[23] For some locations and especially thick multi-layer walls it can however be difficult to accurately read a moisture value. Proposals for in-situ water content sensors have also been made utilizing SAW-based transponders [24].
Previous sections have shown that the performance of low cost tags, constructed with simple one-layer antennas, is very sensitive to the surrounding environment and especially to nearby metallic surfaces. Water is no exception since its relative permittivity is of the order of 80+j×80 and will directly cause ohmic losses in an antennas near-field and also change its resonance frequency. It has previously been characterized as to how this property can be used to measure wetness in soil and snow by connecting a transmission line to a buried monopole antenna [25].
The concept suggested here is based on the use of two tags on one label where one of the tags is embedded in a moisture absorbent material and the other is left open. In a humid environment the moisture concentration is higher in the absorbent material than in the surrounding environment which causes degradation to the embedded tag's antenna in terms of dielectric losses and change of input impedance as water increases both the real and imaginary parts of the paper's dielectric constant [26].
If the tags are passive, an RFID reader held at the same distance from both tags in the label must therefore emit a stronger interrogating signal in order to power up the embedded tag than the naked tag. By comparing the minimum power levels required to power up each tag it is therefore possible to determine the humidity level at the tag's location.
Moisture measurement by embedding an RFID tag could theoretically also be performed using only one tag but that would require the distance and materials between the reader and the embedded tag to always be exactly the same.

8.1.1 Characterizing pair of tags

Two passive 868 MHz Gen-2 tags from Alien using the Alien Squiggle antenna were used in experiments performed in a climate chamber. In three different setups, 10 stacked sheets of blotting papers made out of bleached kraft pulp with a basis weight of 260 g/m^2 were placed respectively in front, behind and both in front and behind one of the tags. A SAMSys RFID reader allowing control of the antenna output power was used with its antenna positioned symmetrically about 1.5 m from the pair of tags.
Results are presented in Fig. 17 (a), which can later be used as a look-up table for humidity levels when measuring labels placed at hidden locations.
The tags were also characterized for direct wetness with the result shown in Fig. 17 (b).

8.1.2 Remarks for the double tag RFID sensor approach

It is observed that the more embedded a tag is the more sensitive it is to the surrounding humidity. The larger total volume of absorbing material in the embedded tag introduces a larger total amount of water near the tag antenna. At 90% RH the half-open and totally embedded tag shows approximately the same difference when compared to the totally open reference tags. The differences in power levels for different levels of relative humidity proved to be of the order of a couple of decibels for the 80 % RH where humidity may become the source of mould. This places significant constraints on the tolerances of the

readout electronics and, additionally, that the individual tag antennas within the label are not externally distorted by small variations in their respective vicinities.

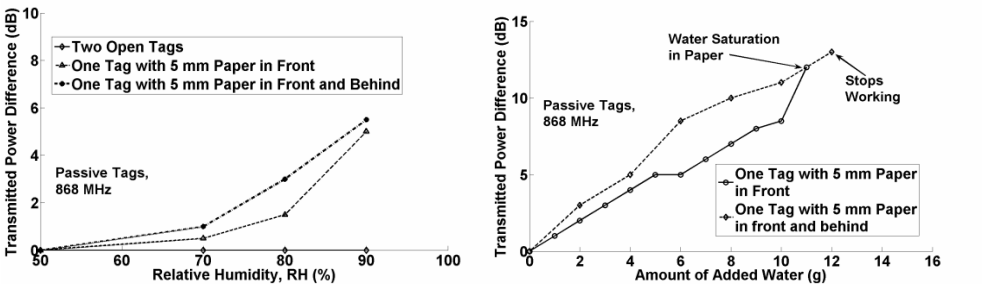

(a) (b)

Fig. 17. Difference in minimum output power required from the RFID reader in order to read two passive tags in a label where one is covered or embedded in a moisture absorbing material.

As is shown in Fig. 17 (b), the tag embedded with 5 mm paper on each side also was not readable at all at 1.61 m when it received more than 12 grams of water. At the time of malfunction the difference in transmitted power was about 13 dB.

It is also observed that the difference in minimum transmitted power is almost linear to the amount of water added. Even though the totally embedded tag shows a greater difference than the tag covered only on one side, the difference for small amounts of water is not significant.

A more advanced label could include three or more tags where perhaps one tag could have its antenna completely dissolved if moisture exceeds a certain value. This could for example be accomplished by having a water based electrically conductive ink (i.e. silver ink). In that way one would create a memory effect that states that the relative humidity has been above a certain level and could also provide the current value.

9. References

[1] K. Finkenzeller, "RFID Handbook", ISBN 0-470-84402-7, John Wiley & Sons 2003

[2] Agilent Technologies, Inc., "HSMS-282x Series - Surface Mount RF Schottky Barrier Diodes" Data Sheet, March 2005, http://pdf1.alldatasheet.com/datasheet-pdf/view/95384/HP/HSMS282X.html, accessed 2009-09-11

[3] Ansoft High Frequency Structure Simulator (HFSS) 9.2, Ansoft Corp. www.ansoft.com, accessed 2009-09-27

[4] D. K. Cheng, "Field and Wave Electromagnetics", 2nd edition, ISBN 0-201-12819-5, Addison Wesley, UK, 1989

[5] H. Tanaka, F. Okada, "Precise Measurements of Dissipation Factor in Microwave Printed Circuit Boards", *IEEE Trans .Instrumentation and Measurement*, vol. 38, no. 2, pp. 509-514, April 1989

[6] Carl Mahr Holding GmbH, www.mahr.com, accessed 090927

[7] C.A. Balanis, "Antenna Theory: Analysis and Design, 2nd ed.", pp. 59, 61, 873, ISBN 0-471-59268-4, John Wiley & Sons 1997

[8] J. I. Kim, B.M. Lee and Y. J. Yoon, "Wideband Printed Dipole Antenna for Multiple Wireless Services", *Applied Microwave & Wireless Magazine*, pp. 70-77, September 2002

[9] Q. Xianming; Y.Ning, "A folded dipole antenna for RFID", *IEEE Int. Symp. Ant. and Prop.*, 2004, Vol. 1, pp. 97 – 100, 2004

[10] P. V. Nikitin, et al., "Power reflection coefficient analysis for complex impedances in RFID tag design," *IEEE Trans. Microw. Theory Tech.*, vol. 53, pp. 2721-2725, 2005

[11] L. Ukkonen, D. Engels, L. Sydänheimo, M. Kivikoski, "Planar wire-type inverted-F RFID tag antenna mountable on metallic objects", *IEEE Int. Symp- Antennas and Propagation 2004*, Vol. 1, pp. 101 – 104, 2004

[12] H. Kwon, B. Lee, "Compact slotted planar inverted-F RFID tag mountable on metallic objects," *Electron. Lett.*, Vol. 41, No. 24, pp. 1308-1310, 2005

[13] L. Ukkonen, M. Schaffrath, L. Sydanheimo and M. Kivikoski, "Analysis of integrated slot-type tag antennas for passive UHF RFID," *IEEE Ant. and Prop. Society Int. Symp.*, pp. 1343-1346, 2006

[14] L. Ukkonen, L. Sydanheimo, M. Kivikoski, "Effects of metallic plate size on the performance of microstrip patch-type tag antennas for passive RFID", *Antennas and Wireless Propagation Letters,* Vol. 4, pp.410 – 413, 2005

[15] H.-W. Son, G.-Y. Choi and C.-S. Pyo, "Design of wideband RFID tag antenna for metallic surfaces," *Electron. Lett.*, Vol. 42, No. 5, pp. 263-265, 2006.

[16] G. Kumar, K. P. Ray, Broadband microstrip antennas, *Artech House*, USA, pp. 205-227, 2003

[17] FlexiProof 100, RK Print Coat Instruments Ltd, *www.rkprint.com*

[18] Precisia, LLC, formerly subsidiary of the Flint Group, www.flintgrp.com, accessed 091013

[19] W. N. Caron "Antenna Impedance Matching", Amer Radio Relay League, June 1989

[20] [Y.L. Chow and C.W. Fung, "The city university logo patch antenna", *Proc. Asia-Pacific Microwave Conference, 1997. APMC '97*, Vol. 1, pp. 229 – 232, Dec. 1997

[21] [M. Keskilammi, M. Kivikoski, "Using text as a meander line for RFID Transponder Antennas", *Antennas and Wireless Propagation Letters*, Vol. 3, Issue 16, pp. 372 – 374, Dec. 2004

[22] F. Menke, R. Knochel, T. Boltze, C. Hauenschild, and W. Leschnik, "Moisture measurement in walls using microwaves", *IEEE Int. Microwave Symp.* 1995, Vol. 3, pp. 1147 – 1150, 1995

[23] T. Hauschild, and F. Menke, "Moisture measurement in masonry walls using a non-invasive reflectometer", *Electronics Letters,* Vol. 34, Issue 25, pp. 2413 – 2414, 1998

[24] L. Reindl, C.C.W. Ruppel, A. Kirmayr, N. Stockhausen, M.A. Hilhorst and J. Balendonckm, "Radio-requestable passive SAW water-content sensor", *IEEE Trans. Microwave Theory and Techniques*, Vol. 49, Issue 4, Part 2, pp. 803 – 808, April 2001

[25] A. Denoth, "The monopole-antenna: a practical snow and soil wetness sensor", *IEEE Trans. Geoscience and Remote Sensing*, Vol. 35, Issue 5, pp. 1371 – 1375, Sept. 1997

[26] L. Apekis, C. Christodoulides, P. Pissis, "Dielectric properties of paper as a function of moisture content", *Dielectric Materials, Measurements and Applications 1988, Fifth Int. Conf. on*, pp. 97 – 100, 1988

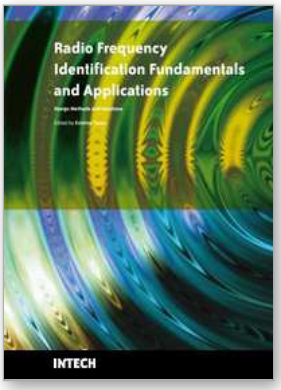

Radio Frequency Identification Fundamentals and Applications
Design Methods and Solutions
Edited by Cristina Turcu

ISBN 978-953-7619-72-5
Hard cover, 324 pages
Publisher InTech
Published online 01, February, 2010
Published in print edition February, 2010

This book, entitled Radio Frequency Identification Fundamentals and Applications, Bringing Research to Practice, bridges the gap between theory and practice and brings together a variety of research results and practical solutions in the field of RFID. The book is a rich collection of articles written by people from all over the world: teachers, researchers, engineers, and technical people with strong background in the RFID area. Developed as a source of information on RFID technology, the book addresses a wide audience including designers for RFID systems, researchers, students and anyone who would like to learn about this field. At this point I would like to express my thanks to all scientists who were kind enough to contribute to the success of this project by presenting numerous technical studies and research results. However, we couldn't have published this book without the effort of InTech team. I wish to extend my most sincere gratitude to InTech publishing house for continuing to publish new, interesting and valuable books for all of us.

INTECH
open science | open minds

InTech Europe
University Campus STeP Ri
Slavka Krautzeka 83/A
51000 Rijeka, Croatia
Phone: +385 (51) 770 447
Fax: +385 (51) 686 166
www.intechopen.com

InTech China
Unit 405, Office Block, Hotel Equatorial Shanghai
No.65, Yan An Road (West), Shanghai, 200040, China
中国上海市延安西路65号上海国际贵都大饭店办公楼405单元
Phone: +86-21-62489820
Fax: +86-21-62489821